

Inhibitors of VEGF receptors-1 and -2 based on the 2-((pyridin-4-yl)ethyl)pyridine template

Alexander S. Kiselyov,^{a,*} Marina Semenova,^b Victor V. Semenov^c and Daniel Milligan^d

^aSmall Molecule Drug Discovery, Chemical Diversity, Inc, 11558 Sorrento Valley Road, San Diego, CA 92121, USA

^bInstitute of Developmental Biology, Russian Academy of Sciences, 26 Vavilov Str., 119334 Moscow, Russia

^cZelinsky Institute of Organic Chemistry, Russian Academy of Sciences, 47 Leninsky Prospect, 117913 Moscow, Russia

^dDepartment of Chemistry, ImClone Systems, 180 Varick Street, New York, NY 10014, USA

Received 30 November 2005; revised 21 December 2005; accepted 22 December 2005

Available online 3 February 2006

Abstract—We have developed a series of novel potent ((pyridin-4-yl)ethyl)pyridine derivatives active against kinases VEGFR-1 and -2. Both specific and dual ATP-competitive inhibitors of VEGFR-2 were identified. Kinase selectivity could be controlled by varying the arylamino substituent at the 1,3,4-oxadiazole ring. The most specific molecules displayed >10-fold selectivity for VEGFR-2 over VEGFR-1. Compound activities in vitro and in cell-based assays ($IC_{50} < 100$ nM) were similar to those of reported clinical and development candidates, including PTK787 (VatalanibTM). High permeability of active compounds across the Caco-2 cell monolayer ($>30 \times 10^{-5}$ cm/min) is indicative of their potential for intestinal absorption upon oral administration.

© 2006 Elsevier Ltd. All rights reserved.

Angiogenesis, or formation of new blood vessels, is a highly complex process. Proliferation and migration of capillary endothelial cells from pre-existing blood vessels is followed by tissue infiltration and cell assembly into tubular structures, joining of newly formed tubular assemblies to closed-circuit vascular systems, and maturation of newly formed capillary vessels. Angiogenesis is involved in pathological conditions such as tumor growth and degenerative eye conditions.¹ Family of vascular endothelial growth factors (VEGFs),² endothelial cell-specific mitogens, has been implicated in regulation of angiogenesis in vivo. VEGFs mediate their biological effect through high affinity VEGF receptors which are expressed on the endothelial cells. These include receptor tyrosine kinases, VEGFR-1 (Flt-1) and VEGFR-2 (kinase insert domain receptor (KDR) or flk1).³ Whereas VEGFR-1 functions are still under investigation, there is evidence that KDR is a major mediator of vascular endothelial cell mitogenesis as well as angiogenesis and microvascular permeability. It is believed that a direct inhibition of the aberrant KDR kinase activity results in reduction of tumor angiogenesis and

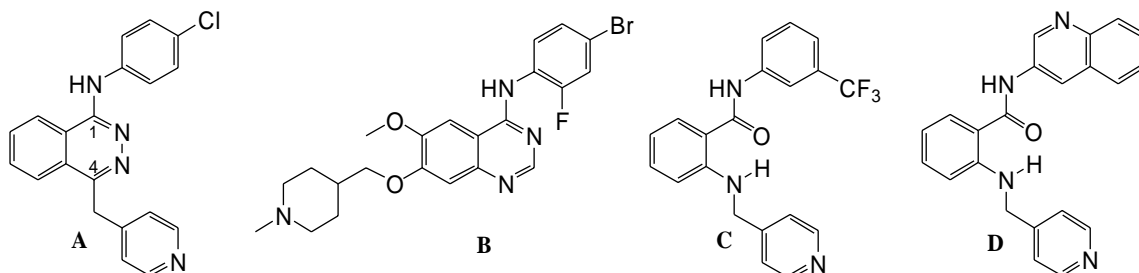
suppression of tumor growth. Potent, specific, and non-toxic inhibitors of angiogenesis are powerful clinical tools in oncology and ophthalmology.³

There are reports describing small-molecule inhibitors that affect VEGF/VEGFR signaling by directly competing with the ATP binding site of the respective intracellular kinase domain. This event leads to the inhibition of VEGFR phosphorylation and, ultimately to apoptotic death of the aberrant endothelial cells. Drug candidates that exhibit this mechanism of action include PTK787 (VatalanibTM, **A**) and ZD6474 (VandetanibTM, **B**). These are phases III and II clinical candidates, respectively, against various cancers.^{4,5} The 6-membered ring of a phthalazine template in PTK787 has been replaced with the isosteric anthranil amide derivatives **C** and **D**. Intramolecular hydrogen bonding was suggested to be responsible for the optimal spatial orientation of pharmacophores, similar to the parent PTK787.⁶

It has been suggested that the essential pharmacophores for the VEGFR-2 activity of phthalazines and their analogues include: (i) [6,6]fused (or related) aromatic system; (ii) *para*- or 3,4-di-substituted aniline function in the position 1 of phthalazine; and (iii) hydrogen bond acceptor (Lewis' base: lone pair(s) of a nitrogen- or oxygen atom(s)) attached to the position 4 via an appropriate linker (aryl or fused aryl group).⁴ In this letter, we

Keywords: Vascular endothelial growth factor receptor 2; VEGFR-2; VEGFR-1; Receptor tyrosine kinase; Dual kinase inhibitors; Angiogenesis; ((Pyridin-4-yl)ethyl)pyridines.

* Corresponding author. E-mail: ask@chemdiv.com



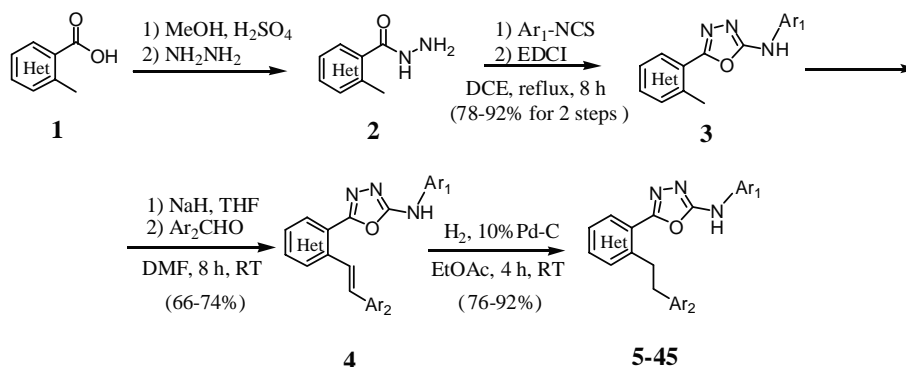
expand upon our initial findings⁷ and disclose potent inhibitors of VEGFR-2 kinase based on a 2-((pyridin-4-yl)ethyl)pyridine core. We reasoned that this non-phthalazine template could provide for the proper pharmacophore arrangement relevant to compounds PTK787, **C** and **D**.

The desired molecules **5–45** were accessed by a four-step reaction sequence shown in **Scheme 1**. Commercially available methyl picolinic or quinolinic acids **1** were refluxed in anhydrous MeOH with catalytic amount of concentrated H₂SO₄ for 1 h followed by the addition of a 15-fold molar excess of anhydrous hydrazine and reflux for an additional 2 h. Removal of solvent and excess hydrazine in vacuo (Caution! Efficient liquid N₂ trap!) was followed by the reaction of the resulting crude hydrazides **2** with a series of aryl thiocyanates (Ar₁-NCS) in dichloroethane at rt for 2 h. Subsequently, the reaction mixtures were treated in situ with EDCI (2.5 equiv) at 0 °C, brought to reflux, and stirred for 8 h to promote heterocyclization of the intermediate thiosemicarbazides. The targeted amino oxadiazoles **3** were conveniently isolated by trituration of the concentrated reaction mixtures with Et₂O followed by re-crystallization of the resulting solids from EtOH (78–92% yields for two steps). The collected crystalline materials **3** were treated with NaH (2.25 equiv) in dry freshly distilled DMF at 0 °C. The resulting anions were reacted at rt with a series of aromatic aldehydes (Ar₂-CHO) for 8 h to yield the respective diaryl olefins **4**. Compound **4** was isolated in 66–74% by column chromatography (eluent: hexanes/EtOAc, 2:1; mixtures of *trans*- and *cis*-isomers (ca. 4:1–5:1)) and hydrogenated without separation in EtOAc for 4 h at rt using 10% Pd/C until both TLC and LC–MS analyses indicated the complete conversion of **4** into the targeted molecules **5–45**. The prod-

ucts were isolated by flash chromatography (eluent: hexanes/Et₂O, 1:1) to afford analytically pure materials in 76–92% yield.⁸

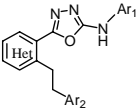
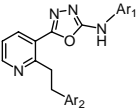
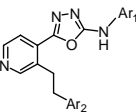
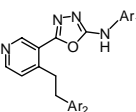
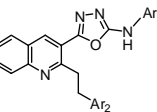
Compounds (**5–45**, **Table 1**) were tested in vitro against isolated VEGFR-2 kinase. Specifically, we measured their ability to inhibit phosphorylation of a biotinylated polypeptide substrate (pGAT, CIS Bio International) in a homogeneous time-resolved fluorescence (HTRF) assay at an ATP concentration of 2 μM. The results were reported as a 50% inhibition concentration value (IC₅₀). Literature VEGFR-2 inhibitors **A–D** (**Table 1**) were included as an internal standards for quality control.^{6,9}

As seen from **Table 1**, a number of ((pyridin-4-yl)ethyl)pyridine derivatives exhibited a robust inhibitory activity against VEGFR-2. By varying both aryl substituents (anilinic groups) on a 1,3,4-oxadiazole function and (arylethyl)pyridine pharmacophores, we modulated the compounds' potency against the enzyme. Initially, we kept the anilinic function constant (3-CF₃-C₆H₄-NH, similar to the compound **C**)^{4,6} and studied the inhibitory effect of an aryethyl group and central pyridine template on the enzymatic activity of the resultant compounds **5–18** (**Table 1**). (Pyridin-4-yl)ethyl derivative **5** furnished the best activity with the IC₅₀ value of 64 nM against VEGFR-2. The respective analogue **17** of the compound **D** (vide supra) showed a considerably weaker enzymatic potency (0.38 μM). In addition, it did not display cellular activity, presumably due to poor cell permeability.¹⁰ Furthermore, the nature of pyridine template was found to have a profound effect on the compounds potency. Molecules based on 3- and 4-pyridine cores consistently displayed weaker activity against VEGFR-2, when compared to the compounds derived



Scheme 1.

Table 1. Activity of ((pyridin-4-yl)ethyl)pyridines and quinolines **5–45** against VEGFR-1 and -2

<div style="display: flex; justify-content: space-around; align-items: center;"> <div style="text-align: center;">  <p>5-45</p> </div> <div> <p>Templates: 2-Py</p> </div> <div style="text-align: center;">  <p>2-Py</p> </div> <div style="text-align: center;">  <p>3-Py</p> </div> <div style="text-align: center;">  <p>4-Py</p> </div> <div style="text-align: center;">  <p>2-Quin</p> </div> </div>						
Compound	Pyridine ring	Ar ₁	Ar ₂	VEGFR-2, enzymatic, IC ₅₀ ^a (μM)	VEGFR-1, enzymatic, IC ₅₀ ^a (μM)	VEGFR-2, cell-based ELISA, IC ₅₀ ^a (μM)
A, PTK787				0.054 ± 0.006 (0.042 ± 0.003)	0.14 ± 0.02 (0.11 ± 0.03)	0.021 ± 0.03 (0.016 ± 0.001)
B, ZD6474				0.022 ± 0.003 (0.017 ± 0.003)	0.10 ± 0.01 (0.09 ± 0.01)	1.66 ± 0.11 (2.70 ± 0.17)
C				0.032 ± 0.005 (0.023 ± 0.006)	0.17 ± 0.05 (0.130 ± 0.081)	0.09 ± 0.01 (0.0012 ± 0.0002)
D				0.015 ± 0.004 (0.009 ± 0.001)	0.16 ± 0.05 (0.13 ± 0.03)	0.05 ± 0.01 (0.0012 ± 0.0001)
5	2-Py	3-F ₃ C(C ₆ H ₄)	4-Pyridine	0.064 ± 0.008	0.22 ± 0.04	0.11 ± 0.02
6	3-Py	3-F ₃ C(C ₆ H ₄)	4-Pyridine	0.56 ± 0.07	0.76 ± 0.08	1.11 ± 0.10
7	4-Py	3-F ₃ C(C ₆ H ₄)	4-Pyridine	0.72 ± 0.07	1.22 ± 0.16	2.54 ± 0.32
8	2-Quin	3-F ₃ C(C ₆ H ₄)	4-Pyridine	>10	>10	>10
9	2-Py	3-F ₃ C(C ₆ H ₄)	3-Pyridine	>10	>10	>10
10	2-Py	3-F ₃ C(C ₆ H ₄)	2-Pyridine	>10	>10	>10
11	2-Py	3-F ₃ C(C ₆ H ₄)	Piperonyl	>10	>10	>10
12	2-Py	3-F ₃ C(C ₆ H ₄)	3,4-Di-F(C ₆ H ₃)	>10	>10	>10
13	3-Py	3-F ₃ C(C ₆ H ₄)	Piperonyl	>10	>10	>10
14	2-Py	3-F ₃ C(C ₆ H ₄)	5-Indazole	3.87 ± 0.30	>10	>10
15	2-Py	3-F ₃ C(C ₆ H ₄)	2-Quinoline	>10	>10	>10
16	2-Py	3-F ₃ C(C ₆ H ₄)	5-Quinoline	5.64 ± 0.51	>10	>10
17	2-Py	3-Quinolino-	4-Pyridine	0.38 ± 0.04	0.44 ± 0.06	N/A ^{b,10}
18	2-Quin	3-Quinolino-	4-Pyridine	>10	>10	ND
19	2-Py	4- <i>t</i> -Bu(C ₆ H ₄)	4-Pyridine	0.043 ± 0.008^c	0.77 ± 0.11	0.063 ± 0.01
20	2-Py	4- <i>i</i> -Pr(C ₆ H ₄)	4-Pyridine	0.051 ± 0.009	0.62 ± 0.10	0.075 ± 0.01
21	3-Py	4- <i>t</i> -Bu(C ₆ H ₄)	4-Pyridine	0.19 ± 0.02	0.22 ± 0.02	0.32 ± 0.03
22	3-Py	4- <i>i</i> -Pr(C ₆ H ₄)	4-Pyridine	0.25 ± 0.03	0.27 ± 0.03	0.39 ± 0.04
23	4-Py	4- <i>t</i> -Bu(C ₆ H ₄)	4-Pyridine	0.31 ± 0.03	0.48 ± 0.04	0.52 ± 0.06
24	2-Quin	4- <i>t</i> -Bu(C ₆ H ₄)	4-Pyridine	>10	>10	ND
25	2-Py	4-ClF ₂ CO(C ₆ H ₄)	4-Pyridine	0.031 ± 0.006	0.73 ± 0.01	0.044 ± 0.007
26	2-Py	4-F ₃ CO(C ₆ H ₄)	4-Pyridine	0.044 ± 0.007	0.56 ± 0.05	0.051 ± 0.007
27	2-Py	4-F ₃ C(C ₆ H ₄)	4-Pyridine	0.058 ± 0.008	0.32 ± 0.05	0.076 ± 0.009
28	3-Py	4-ClF ₂ CO(C ₆ H ₄)	4-Pyridine	0.22 ± 0.02	0.81 ± 0.06	0.53 ± 0.06
29	3-Py	4-F ₃ CO(C ₆ H ₄)	4-Pyridine	0.35 ± 0.04	0.93 ± 0.06	0.66 ± 0.07
30	3-Py	4-F ₃ C(C ₆ H ₄)	4-Pyridine	0.29 ± 0.04	0.84 ± 0.07	0.72 ± 0.08
31	4-Py	4-ClF ₂ CO(C ₆ H ₄)	4-Pyridine	0.44 ± 0.05	0.53 ± 0.06	0.59 ± 0.06
32	4-Py	4-F ₃ CO(C ₆ H ₄)	4-Pyridine	0.36 ± 0.007	0.47 ± 0.05	0.51 ± 0.06
33	4-Py	4-F ₃ C(C ₆ H ₄)	4-Pyridine	0.44 ± 0.04	0.67 ± 0.08	0.74 ± 0.10
34	2-Py	3-F ₃ CO(C ₆ H ₄)	4-Pyridine	0.069 ± 0.009	0.26 ± 0.04	0.11 ± 0.01
35	3-Py	3-F ₃ CO(C ₆ H ₄)	4-Pyridine	0.47 ± 0.05	0.71 ± 0.08	0.86 ± 0.12
36	4-Py	3-F ₃ CO(C ₆ H ₄)	4-Pyridine	0.55 ± 0.06	0.74 ± 0.07	0.76 ± 0.11
37	2-Py	3-Me(C ₆ H ₄)	4-Pyridine	0.77 ± 0.09	1.07 ± 0.11	2.14 ± 0.23
38	2-Py	3-MeO(C ₆ H ₄)	4-Pyridine	0.17 ± 0.02	0.50 ± 0.07	0.29 ± 0.02
39	2-Py	2-MeO(C ₆ H ₄)	4-Pyridine	>10	>10	ND
40	2-Py	2-Me(C ₆ H ₄)	4-Pyridine	>10	>10	ND

(continued on next page)

Table 1 (continued)

Compound	Pyridine ring	Ar ₁	Ar ₂	VEGFR-2, enzymatic, IC ₅₀ ^a (μM)	VEGFR-1, enzymatic, IC ₅₀ ^a (μM)	VEGFR-2, cell-based ELISA, IC ₅₀ ^a (μM)
41	2-Py	3,4-Di-Cl(C ₆ H ₄)	4-Pyridine	0.079 ± 0.008	0.27 ± 0.08	0.094 ± 0.008
42	2-Py	3,4-Di-MeO(C ₆ H ₄)	4-Pyridine	0.067 ± 0.008	0.18 ± 0.04	0.11 ± 0.01
43	2-Py	4-Me-3-CF ₃ (C ₆ H ₃)	4-Pyridine	0.087 ± 0.007	0.12 ± 0.10	0.092 ± 0.01
44	2-Py	Piperonyl-	4-Pyridine	0.085 ± 0.009	0.14 ± 0.02	0.29 ± 0.04
45	2-Py	4-Ph(C ₆ H ₄)	4-Pyridine	2.63 ± 0.40	>10	ND

^a IC₅₀ values were determined from the logarithmic concentration–inhibition curves (ten points). The values are given as means of at least two duplicate experiments. ND, not determined.

^b Cellular activity was not detected.

^c Bold italics indicate compounds that have >10-fold selectivity for VEGFR-2 over VEGFR-1.

from the 2-pyridine scaffold (e.g., compare **5–7**, Table 1). This pattern was observed throughout our structure–activity relationship studies of the title series (e.g., compare **19** and **20** with **21–23** and **25–27** with **28–33**, Table 1). The related 2-quinoline template did not yield enzymatically active compounds, despite the optimized substitution pattern (see entries **8**, **18**, and **24**).

Good inhibitory activity of **5** was explained by the proper alignment of the 4-substituent, namely pyridine-type nitrogen atom (Lewis' base: hydrogen bond acceptor) with the Arg1302 moiety in the ATP binding pocket of VEGFR-2. We further reasoned that in **9** and **10** the nitrogen of the pyridine ring is likely to be misaligned with the Arg1302. Similarly, indazole, 2- and 5-quinoline functions in **14–16** could be too large to fit into a respective binding pocket.¹¹ 2-Pyridyl template may be responsible for picking an additional hydrogen bonding with the amide bond of Val899 improving overall potency of the respective analogues against the kinase. On the contrary, lone nitrogen pair in the derivatives of 3- and 4-pyridine templates may cause unfavorable electrostatic interactions in the ATP binding site of the kinase, as evidenced from the reported binding mode of PTK787 and its analogues to VEGFR2.¹¹ Similarly, 2-quinoline core may be too bulky to be properly accommodated in the binding pocket due to the close proximity of Leu840.MMFF94 Force Field minimization studies suggested good overlap between active series described in this paper and the development candidates PTK787 and **C** (Fig. 1).¹¹ Following these data, we decided to continue optimization of molecules derived from 4-pyridyl aldehyde (**19–45**, Table 1).

In the next step, we focused on studying SAR of the anilinic portion of the molecule attached to the 1,3,4-oxadiazole moiety. The molecules substituted with *para-t*-Bu- and *para-i*-Pr- groups displayed good

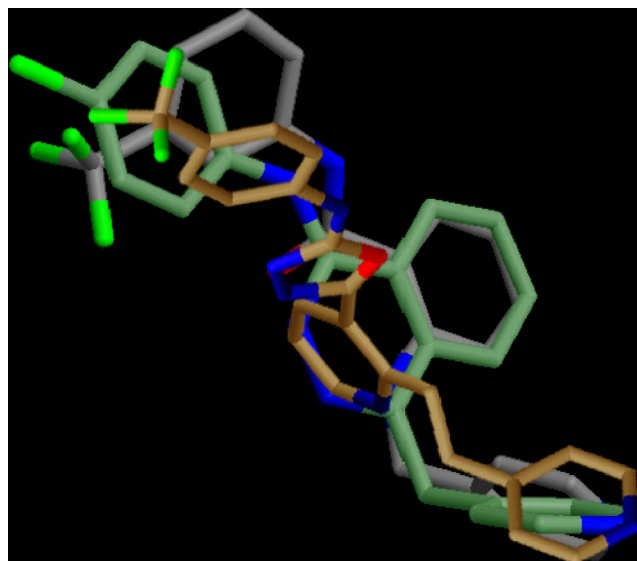


Figure 1. Structural overlap between inhibitor **27** (gold), PTK787 A (green), and **C** (green).

potency with the IC₅₀ values of 43 and 51 nM in the enzymatic assay (e.g., **19** and **20**). The 4-ClF₂CO-group (**25**) resulted in improved activity (IC₅₀ = 31 nM). Both 4-F₃CO- and 4-F₃C-derivatives (**26** and **27**) also inhibited VEGFR-2 (IC₅₀s of 44 and 58 nM). 3-F₃CO- (**34**) and 3-MeO- (**38**) derivatives afforded enzymatic potencies of 69 and 170 nM, respectively. Again, a similar substitution pattern for 3- and 4-pyridine templates yielded compounds with dramatically reduced activities (**35** and **36**; 0.47 and 0.55 μ M, respectively). Small *meta*-substituents resulted in considerably less active molecules (**37**, IC₅₀ = 0.77 μ M). *ortho*-Substitution abolished enzymatic inhibition (**39** and **40**; IC₅₀ > 10 μ M for both). 3,4-Di-substituted aryl groups also yielded potent compounds. Examples include 3,4-di-Cl- (**41**; IC₅₀ = 79 nM), 3,4-di-MeO (**42**, IC₅₀ = 67 nM), 4-Me-3-CF₃- (**43**, IC₅₀ = 87 nM), and piperonyl groups (**44**; IC₅₀ = 85 nM). Larger anilinic substituents also led to the diminished potency against the enzyme (**45**). Specifically, *para*-phenyl- and phenoxy- (data not shown) derivatives displayed weak to no enzymatic activity. We speculated that these functions cannot be properly accommodated in the tight hydrophobic pocket of VEGFR-2.¹¹ Three selected compounds, namely **19**, **25**, and **27** were found to be ATP-competitive inhibitors of VEGFR-2 in the radioassay.¹²

Compounds **5–45** were also tested via HTRF format against VEGFR-1. The results in Table 1 indicate that many VEGFR-2 active ((pyridin-4-yl)ethyl)pyridines display good activity against VEGFR-1 as well. For the most potent compounds, the IC₅₀ values were in 0.14–0.65 μ M range. This outcome could be of benefit in the clinical setting as both receptors are reported to mediate VEGF signaling in angiogenesis.^{1,13} Notably, several compounds containing bulky *para*-substituted anilinic functions at the 1,3,4-oxadiazole pharmacophore (**19**, **20**, **25**, and **26**) yielded over 10-fold selectivity for the VEGFR-2 versus VEGFR-1 kinase. This observation suggests that it is possible to develop VEGFR-2-specific inhibitors lacking VEGFR-1 activity. Structural reasons for this VEGFR-2 specificity are under further investigation. Screening of **5–45** against a number of other receptor (IGF1R, InR, FGFR1, Flt3, ErbB1, ErbB2, and c-Met) and cytosolic (PKA, GSK3 β , PKB/Akt, bcr-Abl, and Cdk2/5) kinases revealed no significant cross-reactivity (PI > 30%, triplicate measurements) at a screening concentration of 10 μ M.

Active in vitro inhibitors of VEGFR-2 were further characterized in a cell-based phosphorylation ELISA (Table 1).¹⁴ In general, good in vitro-to-cell-based activity correlation has been found for these compounds. In our hands, the best compounds displayed 44–110 nM activity in inhibiting cell-based phosphorylation of VEGFR-2. This fact indicates that a number of ((pyridin-4-yl)ethyl)pyridine derivatives, including **19**, **20**, **25–27**, and **41–44**, could be further developed for in vivo studies as both VEGFR-2-specific and VEGFR-1/2-dual inhibitors. High permeability of active compounds across Caco-2 cell monolayer (>30 $\times 10^{-5}$ cm/min) is indicative of their potential for intestinal absorption upon oral administration (Table 2).¹⁰

Table 2. Passive diffusion potential across Caco-2 cell monolayer for selected compounds

Compound	Intrinsic permeability, P_m value $\times 10^{-5}$ cm/min	Absorption potential
C	38.6 (lit. 45.2) ⁶	High
D	17.3 (lit. 21.7) ⁶	Med
5	32.4	High
17	2.7	Low
19	52.7	High
20	42.8	High
25	36.9	High
26	24.7	Med/high
27	43.8	High
28	18.7	Med
30	15.4	Med
34	42.6	High
41	28.7	High
42	25.2	Med/high
43	49.3	High
44	23.6	Med/high

Table 3. Compounds **19**, **25**, and **27** are ATP-competitive inhibitors of VEGFR-2

Compound	K_i at IC ₅₀ (μ M)	K_i at IC ₉₀ (μ M)
19	0.13	0.18
25	0.10	0.08
27	0.12	0.15

In summary, we have developed a series of novel potent ((pyridin-4-yl)ethyl)pyridine derivatives active against kinases VEGFR-1 and -2. Both specific and dual ATP-competitive inhibitors of VEGFR-2 were identified. Kinase selectivity could be controlled by varying the arylamino substituent at the 1,3,4-oxadiazole ring. Several most specific molecules displayed >10-fold selectivity for VEGFR-2 over VEGFR-1. Compound activities in both in vitro and cell-based assays (IC₅₀ < 100 nM) were similar to those of the reported clinical and development candidates, including PTK787 (VatalanibTM). The analogues presented in this letter are potentially useful in the treatment of conditions such as cancer. Further details on their biological properties, such as functional activity, together with murine oral exposure data will be presented in due course (Table 3).

References and notes

- (a) Risau, W. *Nature* **1997**, *386*, 671; (b) Hanahan, D.; Folkman, J. *Cell* **1996**, *86*, 353; (c) Folkman, J.; Klagsburn, M. *Science* **1987**, *235*, 442; (d) Folkman, J. *J. Natl. Cancer Inst.* **1991**, *82*, 4; (e) Kerbel, E. S. *Carcinogenesis* **2000**, *21*, 505.
- (a) Ferrara, N.; Gerber, H.-P.; LeCouter, J. *Nat. Med.* **2003**, *9*, 669; (b) Carmeliet, P.; Jain, R. *Nat. Med.* **2003**, *9*, 653; (c) Veikkola, T.; Karkkainen, M.; Claesson-Welsh, L.; Alitalo, K. *Cancer Res.* **2000**, *60*, 203.
- (a) Klagsbrun, M.; D'Amore, P. *Annu. Rev. Physiol.* **1991**, *53*, 217; (b) Neufeld, G.; Cohen, T.; Gengrinovitch, S.; Poltorak, Z. *FASEB J.* **1999**, *13*, 9; (c) Zachary, I. *Biochem. Soc. Trans.* **2003**, *31*, 1171; (d) Klagsbrun, M.;

- Moses, M. A. *Chem. Biol.* **1999**, *6*, R217; The anti-angiogenic antibody Avastin™ (Bevacizumab) has recently been approved to treat colorectal cancer see (e) Culy, C. *Drugs Today* **2005**, *41*, 23; The anti-angiogenic aptamer Macugen™ (Pegaptanib sodium) has recently been approved to treat neovascular age-related macular degeneration; see (f) Fine, S. L.; Martin, D. F.; Kirkpatrick, P. *Nat. Rev. Drug Disc.* **2005**, *4*, 187.
- Bold, G.; Altmann, K.-H.; Jorg, F.; Lang, M.; Manley, P. W.; Traxler, P.; Wietfeld, B.; Bruggen, J.; Buchdunger, E.; Cozens, R.; Ferrari, S.; Pascal, F.; Hofmann, F.; Martiny-Baron, G.; Mestan, J.; Rosel, J.; Sills, M.; Stover, D.; Acemoglu, F.; Boss, E.; Emmenegger, R.; Lasser, L.; Masso, E.; Roth, R.; Schlachter, C.; Vetterli, W.; Wyss, D.; Wood, J. M. *J. Med. Chem.* **2000**, *43*, 2310.
 - (a) Hennequin, L. F.; Stokes, E. S. E.; Thomas, A. P.; Johnstone, C.; Ple, P. A.; Ogilvie, D. J.; Dukes, M.; Wedge, S. R.; Kendrew, J.; Curwen, J. O. *J. Med. Chem.* **2002**, *45*, 1300; (b) Wedge, S. R.; Kendrew, J.; Hennequin, L. F.; Valentine, P. J.; Barry, S. T.; Brave, S. R.; Smith, N. R.; James, N. H.; Dukes, M.; Curwen, J. O.; Chester, R.; Jackson, J. A.; Boffey, S. J.; Kilburn, L. L.; Barnett, S.; Richmond, G. H. P.; Wadsworth, P. F.; Walker, M.; Bigley, A. L.; Taylor, S. T.; Cooper, L.; Beck, S.; Juergensmeier, J. M.; Ogilvie, D. J. *Cancer Res.* **2005**, *65*, 4389.
 - (a) Manley, P. W.; Furet, P.; Bold, G.; Bruggen, J.; Mestan, J.; Meyer, T.; Schnell, C.; Wood, J. *J. Med. Chem.* **2002**, *45*, 5697; (b) Manley, P. W.; Bold, G.; Fendrich, G.; Furet, P.; Mestan, J.; Meyer, T.; Meyhack, B.; Strauss, A.; Wood, J. *Cell. Mol. Biol. Lett.* **2003**, *8*, 532; (c) Altmann, K.-H.; Bold, G.; Furet, P.; Manley, P. W.; Wood, J. M.; Ferrari, S.; Hofmann, F.; Mestan, J.; Huth, A.; Krüger, M.; Seidelmann, D.; Menrad, A.; Haberey, M.; Thierauch, K.-H., U.S. Patent 6,878,720 B2, 2005.
 - Piatnitski, E. L.; Duncton, M.; Katoch-Rouse, R.; Sherman, D.; Kiselyov, A. S.; Milligan, D.; Balagtas, C.; Wong, W.; Kawakami, J.; Doody, J. *Bioorg. Med. Chem. Lett.* **2005**, *15*, 4696.
 - Analytical data for selected compounds. Compound **24**: *N*-(4-*tert*-butylphenyl)-5-(2-(2-(pyridin-4-yl)ethyl)quinolin-3-yl)-1,3,4-oxadiazol-2-amine; mp 242–244 °C; ¹H NMR (400 MHz, DMSO-*d*₆) δ, ppm: 1.29 (s, 9H, *t*-Bu), 2.86 (m, 2H, CH₂), 3.19 (m, 2H, CH₂), 5.27 (br s, exch D₂O, 1H, NH), 6.52 (d, *J* = 7.2 Hz, 2H), 7.06 (d, *J* = 7.2 Hz, 2H), 7.25 (d, *J* = 5.6 Hz, 2H), 7.42 (m, 1H), 7.66 (m, 1H), 7.72 (d, *J* = 7.6 Hz, 1H), 7.95 (d, *J* = 7.6 Hz, 1H), 8.14 (s, 1H), 8.69 (d, *J* = 5.6 Hz, 2H); ¹³C NMR (100 MHz, DMSO-*d*₆) δ, ppm: 30.8, 33.8, 38.2, 39.7, 107.3, 115.3, 122.9, 124.8, 125.4, 125.7, 126.5, 127.0, 127.9, 128.2, 129.3, 132.1, 134.6, 139.5, 139.8, 144.8, 148.3, 149.5, 159.7, 164.4; ESI MS (M+1): 451, (M–1): 449; HRMS, exact mass calcd for C₂₈H₂₇N₅O: 449.2216. Found: 449.2208. Elemental analysis: calcd for C₂₈H₂₇N₅O: C, 74.81; H, 6.05; N, 15.58. Found: C, 74.59; H, 5.87; N, 15.33.
Compound **27**: 5-(2-(2-(pyridin-4-yl)ethyl)pyridin-3-yl)-*N*-(4-(trifluoromethyl)phenyl)-1,3,4-oxadiazol-2-amine; mp 211–213 °C; ¹H NMR (400 MHz, *c*DMSO-*d*₆) δ, ppm: 2.94 (m, 2H, CH₂), 3.36 (m, 2H, CH₂), 5.35 (br s, exch D₂O, 1H, NH), 6.62 (d, *J* = 7.2 Hz, 2H), 7.11 (dd, *J*₁ = 8.0 Hz, *J*₂ = 4.8 Hz, 1H), 7.19 (d, *J* = 7.2 Hz, 2H), 7.33 (d, *J* = 5.2 Hz, 2H), 7.95 (d, *J* = 8.0 Hz, 1H), 8.55 (d, *J* = 5.2 Hz, 2H), 8.73 (d, *J* = 4.8 Hz, 1H); ¹³C NMR (100 MHz, DMSO-*d*₆) δ, ppm: 33.5, 38.0, 108.5, 115.9, 120.6, 122.2, 123.7, 124.6, 125.9, 130.1, 133.8, 145.2, 146.0, 148.3, 148.9, 156.7, 165.3; ESI MS (M+1): 412, (M–1): 410; HRMS, exact mass calcd for C₂₁H₁₆F₃N₅O: 411.1307. Found: 411.1302. Elemental analysis: calcd for C₂₁H₁₆F₃N₅O: C, 61.31; H, 3.92; N, 17.02. Found: C, 61.12; H, 4.06; N, 16.88.
Compound **30**: 5-(3-(2-(pyridin-4-yl)ethyl)pyridin-4-yl)-*N*-(4-(trifluoromethyl)phenyl)-1,3,4-oxadiazol-2-amine; mp 226–228 °C; ¹H NMR (400 MHz, DMSO-*d*₆) δ, ppm: 2.72 (m, 2H, CH₂), 2.96 (m, 2H, CH₂), 5.28 (br s, exch D₂O, 1H, NH), 6.66 (d, *J* = 7.2 Hz, 2H), 7.24 (d, *J* = 5.2 Hz, 2H), 7.22 (d, *J* = 7.2 Hz, 2H), 7.53 (d, *J* = 4.8 Hz, 1H), 8.48 (d, *J* = 5.2 Hz, 2H), 8.61 (s, 1H), 8.70 (d, *J* = 4.8 Hz, 1H); ¹³C NMR (100 MHz, DMSO-*d*₆) δ, ppm: 29.9, 36.4, 106.2, 116.3, 118.5, 120.7, 122.6, 124.3, 125.4, 137.2, 142.7, 145.9, 147.0, 148.3, 149.1, 149.5, 163.8; ESI MS (M+1): 412, (M–1): 410; HRMS, exact mass calcd for C₂₁H₁₆F₃N₅O: 411.1307. Found: 411.1298. Elemental analysis: calcd for C₂₁H₁₆F₃N₅O: C, 61.31; H, 3.92; N, 17.02. Found: C, 61.07; H, 4.11; N, 16.81.
Compound **33**: 5-(4-(2-(pyridin-4-yl)ethyl)pyridin-3-yl)-*N*-(4-(trifluoromethyl)phenyl)-1,3,4-oxadiazol-2-amine; mp 218–220 °C; ¹H NMR (400 MHz, DMSO-*d*₆) δ, ppm: 2.84 (m, 2H, CH₂), 2.95 (m, 2H, CH₂), 5.33 (br s, exch D₂O, 1H, NH), 6.59 (d, *J* = 7.2 Hz, 2H), 7.23 (d, *J* = 5.2 Hz, 2H), 7.28 (d, *J* = 7.2 Hz, 2H), 7.39 (d, *J* = 4.8 Hz, 1H), 8.53 (d, *J* = 5.2 Hz, 2H), 8.66 (d, *J* = 4.8 Hz, 1H), 8.87 (s, 1H); ¹³C NMR (100 MHz, DMSO-*d*₆) δ, ppm: 29.5, 36.6, 106.1, 115.9, 120.6, 122.9, 124.5, 124.9, 125.7, 132.4, 145.9, 147.0, 148.5, 149.1, 149.6, 150.8, 164.1; ESI MS (M+1): 412, (M–1): 410; HRMS, exact mass calcd for C₂₁H₁₆F₃N₅O: 411.1307. Found: 411.1301. Elemental analysis: calcd for C₂₁H₁₆F₃N₅O: C, 61.31; H, 3.92; N, 17.02. Found: C, 61.15; H, 3.75; N, 16.86.
 - VEGFR-2 kinase inhibition was determined by measuring the phosphorylation level of poly-Glu-Ala-Tyr-biotin (pGAT-biotin) peptide in the HTRF assay. Into a 96-well Costar plate was added 2 μl/well of 25× compound in a 100% DMSO (final concentration in the 50 μl kinase reaction was typically 1 nM to 10 μM). Next, 38 μl of reaction buffer (25 mM Hepes, pH 7.5, 5 mM MgCl₂, 5 mM MnCl₂, 2 mM DTT, and 1 mg/ml BSA) containing 0.5 mmol pGAT-biotin and 3–4 ng KDR enzyme was added to each well. After 5–10 min preincubation, the kinase reaction was initiated by the addition of 10 μl of 10 μM ATP in the reaction buffer, after which the plate was incubated at room temperature for 45 min. The reaction was stopped by addition of 50 μl KF buffer (50 mM Hepes, pH 7.5 and 0.5 M KF, and 1 mg/ml BSA) containing 100 mM EDTA and 0.36 μg/ml PY20K (Eu-cryptate labeled anti-phosphotyrosine antibody, CIS Bio International) was added and after an additional 2 h incubation at rt, the plate was analyzed in a RUBYstar HTRF Reader.
 - Poor passive diffusion potential (intrinsic permeability, *P*_m = 2.7 × 10^{−5} cm/min) for **17** across Caco-2 cell monolayer was predictive of poor cell permeability. In general, good correlation between cell-based activity and *P*_m values was observed for all active compounds (Table 2).
 - (a) McTigue, M. A.; Wickersham, J. A.; Pinko, C.; Showalter, R. E.; Parast, C. V.; Tempczyk-Russell, A.; Gehring, M. R.; Mroczkowski, B.; Kan, C. C.; Villafranca, J. E.; Appelt, K. *Structure* **1999**, *7*, 319; (b) Berman, H. M.; Westbrook, J.; Feng, Z.; Gilliland, G.; Bhat, T. N.; Weissig, H.; Shindyalov, I. N.; Bourne, P. E. *Protein Data Bank, Nucleic Acids Res.* **2000**, *28*, 235.
 - Competition assays were conducted with varying concentrations (0–100 μM) of ATP. Specifically, five different concentrations of ³²P ATP were incubated with VEGFR-2 in the absence, IC₅₀ or IC₉₀ concentration of the inhibitors for 45 min at RT. A double reciprocal graph of the degree of phosphorylation (1/cpm) against ATP concentration (1/[ATP]) was plotted. The data were analyzed by a non-linear least-squares program to determine kinetic

parameters using GraphPad software. Determined K_i values for the three selected compounds are listed in Table 3.

13. Eskens, F. *Br. J. Cancer* **2004**, 90, 1.
14. Cell-based assay for VEGFR-2 inhibition: (i) Transfection of 293 cells with DNA expressing FGFR1/VEGFR-2 chimera: a chimeric construct containing the extracellular portion of FGFR1 and the intracellular portion of VEGFR-2 was transiently transfected into 293 adenovirus-transfected kidney cells. DNA for transfection was diluted to a 5 µg/ml final concentration in a serum-free medium and incubated at room temperature for 30 min with 40 µl/ml of Lipofectamine 2000, also in serum-free media. Two hundred and fifty microliters of the Lipofectamine/DNA mixture was added to 293 cells suspended at 5×10^5 cells/ml. Suspension (200 µl/well) was added to a 96-well plate and incubated overnight. Within 24 h, media were removed and 100 µl of media with 10% fetal bovine serum was added to the now adherent cells followed by an additional 24 h incubation. Test compounds were added to the individual wells (final DMSO concentration was 0.1%). Cells were lysed by re-suspension in 100 µl lysis buffer (150 mM NaCl, 50 mM Hepes, pH 7.5, 0.5% Triton X-100, 10 mM NaPPi, 50 mM NaF, and 1 mM Na_3VO_4)

and rocked for 1 h at 4 °C. (ii) ELISA for detection of tyrosine-phosphorylated chimeric receptor: 96-well ELISA plates were coated using 100 µl/well of 10 µg/ml of αFGFR1 antibody and incubated overnight at 4 °C. αFGFR1 was prepared in a buffer made with 16 ml of a 0.2 M Na_2CO_3 and 34 ml of a 0.2 M NaHCO_3 with pH adjusted to 9.6. Concurrent with lysis of the transfected cells, αFGFR1 -coated ELISA plates were washed three times with PBS + 0.1% Tween-20, blocked by addition of 200 µl/well of a 3% BSA in PBS for 1 h, and washed again. Lysate (80 µl) was then transferred to the coated and blocked wells, and incubated for 1 h at 4 °C. The plates were washed three times with PBS + 0.1% Tween 20. To detect bound phosphorylated chimeric receptor, 100 µl/well of anti-phosphotyrosine antibodies (RC20:HRP), Transduction Laboratories was added (final concentration 0.5 µg/ml in PBS) and incubated for 1 h. The plates were washed six times with PBS + 0.1% Tween-20. Enzymatic activity of HRP was detected by adding 50 µl/well of equal amounts of the Kirkegaard & Perry Laboratories (KPL) substrates A and B. The reaction was stopped by addition of 50 µl/well of a 0.1 N H_2SO_4 and absorbance was measured at 450 nm.